Studies of the Excited State Dynamics of N_2O_2 by Dissociative Photodetachment of $N_2O_2^-$

Runjun Li[†] and Robert E. Continetti*

Department of Chemistry and Biochemistry, University of California, San Diego, 9500 Gilman Drive, La Jolla, California 92093-0340

Received: August 28, 2001; In Final Form: December 4, 2001

The excited states of N_2O_2 have been characterized by studies of the dissociative photodetachment of $N_2O_2^-$ at 266 nm. Photoelectron−photofragment coincidence spectroscopy reveals the correlation between features observed in the photoelectron spectrum and different neutral dissociation pathways. Evidence for at least two isomers of $N_2O_2^-$ is presented and upper limits for their stabilities are determined. One isomer, $ONNO^-$, is stable relative to NO + NO + e^- by $< 1.70 \pm 0.05$ eV, while the second isomer, trigonal $N_2O_2^-$, is stable relative to O^- + N_2O by $< 0.57 \pm 0.05$ eV. The observed dissociation channels are assigned to ONNO → NO + NO, $N_2O_2 \rightarrow O(^3P) + N_2O$, and either $O(^1D) + N_2O$ or $N(^4S) + NO_2$. No evidence for stable N_2O_2 was found, and the dissociation dynamics of the excited states of N_2O_2 are discussed.

1. Introduction

The oxides of nitrogen play an important role in atmospheric chemistry and have received attention owing to their potential importance as intermediates in catalytic reduction processes[1,2] and as potential energetic materials.[3] The weakly bound ground-state dimer of nitric oxide, $(NO)_2$, has been extensively investigated experimentally[4−8] and theoretically.[9−11] Excited states of N_2O_2 have been proposed as intermediates in the reactions of N + NO_2,[12,13] O + N_2O,[14−17] and the efficient vibrational energy transfer processes observed in the self-relaxation of vibrationally excited NO.[18] A number of theoretical studies have predicted the existence of several high energy N_2O_2 isomers,[1,3,19−22] and some experimental studies have sought to characterize these N_2O_2 species.[7,8,18,23,24] In the present study, dissociative photodetachment (DPD) of isomeric forms of $N_2O_2^-$ has been used to both characterize the predissociative excited states of N_2O_2 and to determine the relative energetics of the isomers of $N_2O_2^-$ produced by electron impact on a beam of N_2O.

Using photoelectron spectroscopy of negative ions, Posey and Johnson[25] found evidence for three distinct isomers of $N_2O_2^-$ by varying ion source reagents and conditions. These isomers were produced in the gas phase by electron impact on a supersonic expansion of different gas mixtures. A weakly bound $O_2^-\cdot N_2$ anion was formed from a 5% O_2/N_2 gas mixture, $O^-\cdot N_2O$ (or $N_2O_2^-$) from N_2O, and a weakly bound dimer $NO^-\cdot NO$ was obtained from a 10% NO/Ar mixture. Photoelectron spectra were used to identify these three distinguishable isomers. Matrix isolation spectroscopy experiments have established the existence of C_{2v}-$N_2O_2^-$ and *cis*- or *trans*-$ONNO^-$ anions.[26,27] More recently, Arnold and Neumark characterized the metastable, high-energy forms of neutral N_2O_2 by photoelectron spectroscopy of the $N_2O_2^-$ anion at 266 and 213 nm.[23] Vibrationally resolved progressions corresponding to transitions to several electronic states of the N_2O_2 molecule were observed. Franck−Condon simulations were used to interpret these spectra in terms of a trigonal N_2O_2 species. In addition, studies of the repulsive states of $N_2O_2^-$ were performed by photofragment translational spectroscopy by Osborn, et al.[28]

In studies of gas-phase electron-impact on N_2O, the formation of $N_2O_2^-$ has been proposed to proceed by formation of O^- from dissociative electron attachment to N_2O followed by addition to N_2O and three-body stabilization of the resulting $N_2O_2^-$.[25] Since the reaction of O^- with N_2O can occur by attack of O^- on either the central or terminal nitrogen atom of N_2O, isomeric forms of $N_2O_2^-$ are expected to be formed as intermediates in this reaction. Isotope-labeled experiments[29−31] on this reaction showed that all possible NO^- products are formed with equal probability, indicating that complete isotope scrambling is achieved within the reaction complex, regardless of whether trigonal $N_2O_2^-$ or *trans*- or *cis*-$ONNO^-$ are formed in the initial attack of O^- on N_2O. One purpose of the present work was to search for distinct strongly bound isomers of $N_2O_2^-$ in the gas phase.

Many of the theoretical studies of N_2O_2 have focused on the ground and low-lying excited states of the weakly bound neutral dimer, $(NO)_2$.[32,33] There have also been a number of ab initio calculations focusing on excited-state N_2O_2 isomers,[3,19−22] including the most recent large-basis-set configuration-interaction calculations of Vincent et al.[1] Depending on the level of theory used, the kinetic stabilities and energetics of the excited-state isomers with respect to the NO+NO asymptote vary dramatically. Neumark and co-workers carried out calculations on both triplet and singlet excited states of trigonal N_2O_2, as well as $N_2O_2^-$.[23,28] High-level calculations on both the anionic and neutral states of N_2O_2 have also been reported by Snis and Panas, including the structure and energetics of *cis*- and *trans*-$ONNO^-$ and trigonal C_{2v}-$N_2O_2^-$ anions using DFT/B3LYP and CASPT2 techniques with large basis sets.[9] They predicted that the trigonal C_{2v}-$N_2O_2^-$ species is bound by 1.4 eV, while the *trans*-$ONNO^-$ ion is the most stable form, bound by 1.7 eV relative to NO + NO^-.

In the present experiments, the DPD of $N_2O_2^-$ was studied using photoelectron−photofragment coincidence (PPC) spectroscopy. Measurements of the photoelectron and photofragment kinetic energies in coincidence provide information concerning the mechanism of anion photodetachment and dissociation of

* Corresponding author. E-mail: rcontinetti@ucsd.edu
[†] Current Address: Department of Atmospheric Sciences, Texas A&M University, College Station, TX 77843.

10.1021/jp013330u CCC: $22.00
Published on Web 01/30/2002

the nascent neutral species. $N_2O_2^-$ was produced by electron impact on N_2O. Two major DPD channels,

$$N_2O_2^- + h\nu \rightarrow O + N_2O + e^- \quad (1)$$

$$\rightarrow NO + NO + e^- \quad (2)$$

were observed at 266 nm (4.66 eV). The coincidence measurements allow the photoelectron spectra to be resolved into contributions from different product channels and determination of the dissociation dynamics of the excited states of N_2O_2 accessed in these experiments. A consideration of the energetics of dissociation channels (1) and (2) provides insights into the energetics of isomeric $N_2O_2^-$ and $ONNO^-$.

2. Experimental Section

The apparatus has been previously described in detail[34,35] and is only briefly reviewed here. In these experiments a fast (3−4 keV) mass-selected anion beam is used to carry out photoelectron and photofragment translational spectroscopy in coincidence. Ions are formed by crossing a pulsed supersonic expansion of 10% N_2O/Ar with a 1 keV electron beam at a repetition rate of 1 kHz. The anions pass through a skimmer, are accelerated, and mass-selected by time-of-flight (TOF).

The $N_2O_2^-$ anions are intersected at a right angle with a linearly polarized laser pulse from the fourth harmonic 266 nm (4.66 eV) of a mode-locked, Q-switched, cavity-dumped Nd:YAG laser. This laser produces ∼100 ps fwhm pulses with ∼30 μJ at 266 nm focused to a 0.5 mm spot, and in the data presented here the electric vector of the laser was parallel to the ion beam direction. The recoiling photoelectrons are detected by a time- and position-sensitive detector. The electron laboratory kinetic energy is determined by TOF and the recoil angle by detected position. Measurement of the electron recoil angle allows correction for Doppler broadening due to the fast ion beam. With this correction, the electron kinetic energy (eKE) in the center-of-mass (CM) is determined. The photoelectron spectra are recorded in coincidence with photofragments or stable neutral products in these experiments. The photoelectron spectrometer was calibrated by photodetachment of O^- and I^-, with an eKE resolution $\Delta E/E$ (fwhm) ∼4%.

Photofragments from the ion-laser interaction travel over a 96 cm flight path to a 4-cm-diameter particle detector. Residual ions and any ionic photofragments are removed from the beam by electrostatic deflection. The photofragment detector is composed of a microchannel-plate-assembly coupled to two wedge-and-strip anodes, allowing the time and position-of-arrival of two photofragments to be recorded per laser shot. The time and position information allows direct determination of the photofragment velocities in the center-of-mass (CM) frame. Conservation of linear momentum in the CM frame serves to determine the photofragment mass ratio, ensuring that photofragments originate from a single dissociation event. No evidence for the production of stable N_2O_2 or three-body dissociation processes was observed. The translational energy resolution of the apparatus $\Delta E/E$ (fwhm) is ≤10%. Correlation of the photoelectron with the photofragments is ensured by carrying out the experiment at a low event rate of ∼0.1 event per laser shot, with an estimated false coincidence rate in these experiments of ∼4%.

3. Results

A. Photofragment Mass Spectrum. The photofragment mass distribution obtained in the DPD of $N_2O_2^-$ at 266 nm is shown in Figure 1. The mass spectrum is consistent with at least two product channels, (1) NO + NO + e^- and (2) O + N_2O + e^-. With the mass resolution of $m/\Delta m \approx 10$, the presence of small branching ratios to the $O_2 + N_2 + e^-$ and in particular the N + NO_2 + e^- channels cannot be ruled out, as further discussed below. The apparent O + N_2O + e^- channel is only 6% of the total, as calculated by the peak areas in Figure 1. This is a lower bound for the true branching ratio between these two channels, as there is a lower acceptance of the particle detector for events with asymmetric product mass ratios.

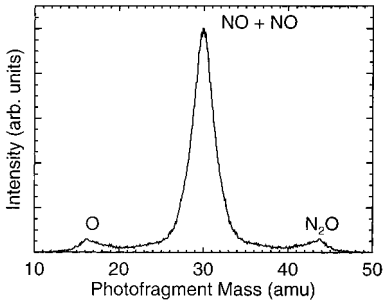

Figure 1. Photofragment mass spectrum for the DPD of $N_2O_2^-$ at 266 nm.

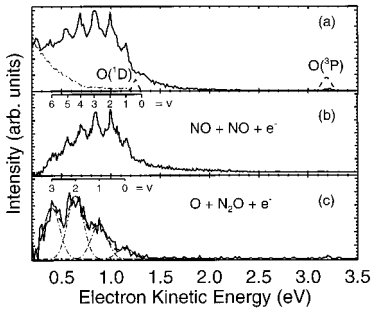

Figure 2. (a) Photoelectron spectrum recorded for photoelectrons plus at least one neutral photofragment at 266 nm (4.66 eV). The dashed line represents a Gaussian fit to the photoelectron spectrum of O^-. No laser background is subtracted from this spectrum; however, the form of the background is shown as the dot−dashed line. (b) Photoelectron spectrum for the NO + NO + e^- product channel. A vibrational progression is labeled and the laser background is subtracted. (c) Photoelectron spectrum for the O + N_2O + e^- product channel. The dashed lines represent the Gaussian fit to the experimental data with fixed width and position. Four broad peaks marked by 0, 1, 2, and 3 are fit by a series of Gaussian functions with fixed width.

B. Photoelectron N(eKE) and Photofragment N(E_T) Spectra. A raw N(eKE) photoelectron spectrum is shown in Figure 2a. This is a total spectrum for both product channels and results from photoelectrons observed in coincidence with at least one photofragment. The peak positions are consistent with the high-resolution photoelectron study of Arnold et al.[23] The rising background at low eKE in Figure 2a is generated by scattered photons interacting with surfaces in the detector region. This background peaks at low energy and falls off rapidly, with little contribution at eKE > 0.7 eV. The peak located at ≈ 3.20 eV corresponds to the photodetachment of $O^-(^2P)$, indicating that some photodissociation of $N_2O_2^-$ ($N_2O_2^- + h\nu \rightarrow O^- + N_2O$) occurs at this wavelength, followed by photodetachment of O^- by a second photon.[23,25] The photodetachment of O^- at 266 nm yields two peaks: at 3.20 and 1.23 eV for the products $O(^3P)$ and $O(^1D)$, respectively. The $O(^1D)$ peak at ≈ 1.23 eV is barely seen as a small shoulder due to the $N_2O_2^-$ photoelectron signal in that region.

Figure 2b shows the photoelectron spectrum recorded in coincidence with two momentum-correlated NO products. This

spectrum has been corrected for laser-generated photoelectron background, which is also reduced by enforcing coincidence with two momentum-matched products. Figure 2c shows the photoelectron spectrum recorded in coincidence with $O + N_2O$ products. The O^- peaks are eliminated in Figure 2b since these data are coincident with NO + NO products; however, the peak related to $O(^3P)$ at 3.20 eV is still evident in Figure 2c as expected, given that this spectrum represents coincidences between $O + N_2O + e^-$.

The photoelectron spectrum of the $NO + NO + e^-$ channel in Figure 2b exhibits a vibrational progression with a frequency of $\omega_e = 1290 \pm 80$ cm^{-1}, consistent with the value of one of the several modes resolved in the higher resolution photoelectron spectra reported by Arnold and Neumark at 1240 ± 10 cm^{-1}. The vibrational band origin is at eKE = 1.31 eV, which is shifted by one vibrational quantum (possibly a vibrational hot band) to larger eKE compared to the results of Arnold and Neumark,[23] corresponding to an adiabatic detachment energy (ADE) of 3.35 eV for this anion. Arnold and Neumark assigned the 1240 cm^{-1} mode to an N−O stretch in a $^3A_2$ state of trigonal C_{2v}-N_2O_2 based on ab initio calculations and Franck−Condon simulations. However, at the highest level of theory carried out, MP2/6-31+G, the calculated vibrational frequency for this mode was 1431 cm^{-1}, considerably larger than the experimental value. Since these photoelectrons are correlated only with NO + NO products and given the energetics discussed below, we propose that an $ONNO^-$ isomer is responsible for this spectrum. Excited states of N_2O_2 have recently been studied by Vincent et al.,[1] who reported the energetics and vibrational frequencies for a number of isomers. They found several structures with vibrational frequencies in the 1250 ± 100 cm^{-1} range. In particular, cyclic ONNO and NONO structures were found that could undergo facile dissociation to NO + NO. Of these, only the cyclic ONNO species would be expected to have significant Franck−Condon overlap with either the *trans*- or *cis*-$ONNO^-$ structures predicted by Snis and Panas.[9] Vincent et al. calculated the cyclic ONNO species to lie 1.66 eV about $NO + NO + e^-$, with an 1100 cm^{-1} symmetric NO stretch.

The photoelectron spectrum of the $O + N_2O + e^-$ channel is located in the low eKE area with strong laser background, and the signal-to-noise suffers from the small branching ratio for this dissociation channel. It is obvious, however, that the photoelectron spectrum coincident with $O + N_2O$ is different from that found for NO + NO products. Four poorly resolved peaks are fit in Figure 2c using Gaussian functions. The peak positions are at 1.14, 0.88, 0.64, and 0.40 eV, consistent with a vibrational progression of $\omega_e \sim 2100$ cm^{-1}. Given the signal-to-noise of this spectrum, this assignment is clearly tentative. The only modes consistent with such a large vibrational spacing are the N−N stretches in trigonal or nearly trigonal N_2O_2 species. Arnold and Neumark calculated 2190 cm^{-1} at the MP2/6-31+G level for the N−N stretch in the C_s symmetry $^1A'$ state of N_2O_2.[23] From the highest energy peak in the photoelectron spectrum, an ADE of 3.52 eV is found for this species.

The photofragment translational energy release spectra, $N(E_T)$, for the two product channels are shown in Figure 3. The spectrum labeled $N(E_T)$ for the $NO + NO + e^-$ products is a broad peak with the most probable E_T at 1.05 ± 0.02 eV. The $N(E_T)$ spectrum for the $O + N_2O + e^-$ products clearly shows two components: a low E_T component at ≈ 0.1 eV and a high E_T component at 0.82 eV ± 0.02.

C. N(E_T,eKE) Correlation Spectra. The measurement of three-particle coincidence events provides a correlation spectrum between E_T and eKE. The correlation spectra $N(E_T,eKE)$ for $NO + NO + e^-$ and $O + N_2O + e^-$ channels are shown by the contour maps in Figures 4 and 5, respectively. The lowest contour line is at 4% of the peak, the false coincidence rate expected in this experiment. No effort has been made to correct for the energy and angular acceptance of the particle detectors

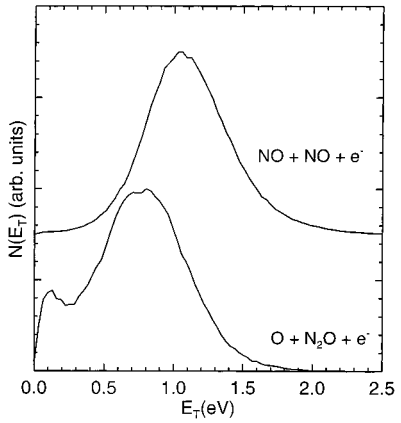

Figure 3. Photofragment translational energy release ($N(E_T)$) spectra for the $NO + NO + e^-$ and the $O + N_2O + e^-$ DPD channels.

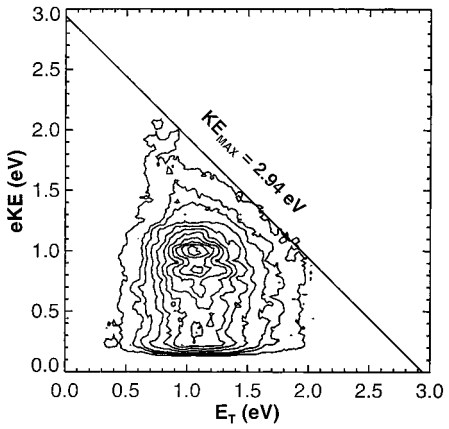

Figure 4. Photoelectron−photofragment ($N(E_T,eKE)$) correlation spectrum (30 000 events) for $N_2O_2^- + h\nu \rightarrow NO + NO + e^-$ at 266 nm, recorded at a beam energy of 4 keV. The assigned maximum kinetic energy for the photoelectron and photofragments, $KE_{max} = 2.94$ eV, is shown as the solid diagonal line. The lowest contour is at the 4% level with the rest of the contours linearly spaced from 10% to 95%.

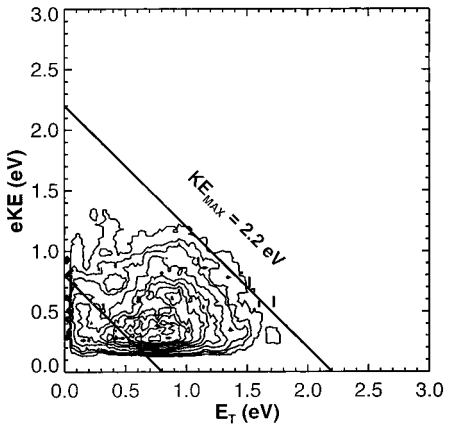

Figure 5. Photoelectron−photofragment ($N(E_T,eKE)$) correlation spectrum (2700 events) for $N_2O_2^- + h\nu \rightarrow O + N_2O + e^-$ at 266 nm (4.66 eV). The assigned maximum kinetic energy for $O(^3P) + N_2O$ is shown as the solid diagonal line at $KE_{max} = 2.2$ eV. In addition, a dashed diagonal line at 0.8 eV is shown for the low-E_T channel discussed in the text. The contours are as in Figure 4.

or laser-correlated background in these spectra, as this is difficult to do with the coincidence spectra.

In Figure 4, horizontal features are seen in the contour map correlated with the peaks in the photoelectron spectrum for NO + NO + e^-. These bands peak at $E_T \sim 1.1$ eV, as seen in the $N(E_T)$ spectrum for this channel in Figure 3. The diagonal line on this spectrum, drawn at the 4% false coincidence level contour represents the maximum kinetic energy release for this DPD process at $KE_{max} = 2.94 \pm 0.05$ eV. The contour map in Figure 5 consists of a low E_T and a high E_T component, corresponding to the two features in the $N(E_T)$ spectrum for O + N_2O + e^- in Figure 3. Two KE_{MAX} values are noted on this figure, $KE_{max} = 2.2 \pm 0.05$ eV for $O(^3P)$ + N_2O + e^- and a second KE_{max} at 0.8 ± 0.05 eV for the low-E_T channel.

4. Discussion

A. Lifetime of the Dissociative States of N_2O_2. The observation of resolved structure in the photoelectron spectra indicates that the dissociative states of N_2O_2 survive for more than a vibrational period. To determine the upper limit of the lifetime for the N_2O_2 dissociative states, we also measured the photofragment translational energy distributions at different beam energies (3 and 4 keV). No difference was found in the measured E_T distributions, indicating that the neutral N_2O_2 dissociated promptly relative to the 9.7 and 8.4 μs flight times from the interaction region to the detector at 3 and 4 keV, respectively. Monte Carlo simulations indicate that an upper limit to the excited-state lifetime is 500 ns, as differences in the observed translational energy distributions would be observed for longer lifetimes. Product angular distributions were also measured for both channels. It was found that for the NO + NO + e^- channel the products were distributed isotropically at low E_T up to the peak of the $N(E_T)$ distribution at 1.05 eV, while the products were peaked along the electric vector of the laser beyond that value. Energy conservation dictates that the products at higher E_T predominantly arise from more highly internally excited N_2O_2 molecules (i.e., lower eKE) and implies that the dissociation lifetime decreases with internal excitation. The O + N_2O product channel is peaked along the electric vector of the laser over the entire translational energy distribution. These results suggest that the more highly excited N_2O_2 internal states dissociate on the order of a rotational period, much faster than the crude upper limit of 500 ns. In any case, no excited states of N_2O_2 were observed with lifetimes useful for energetic materials applications.

B. Energetics. The stability and nature of the anions that have been photodetached is an important aspect of this study. Figure 2 shows that the NO + NO + e^- and O + N_2O + e^- DPD channels are characterized by different photoelectron spectra, consistent with the formation of isomeric forms of $N_2O_2^-$ by electron impact on N_2O. Two isomers of $N_2O_2^-$, trigonal $N_2O_2^-$ and a *trans*- or *cis*-$ONNO^-$ species, are expected to form by this mechanism. The $N(E_T,eKE)$ spectra allow determination of the energetics of the anion precursors, since the relative energetics of the neutral products are well known. Given the photon energy of 4.66 eV, the values for KE_{max} discussed above for these two DPD processes indicate that there are two different anion precursors. This discussion will refer to these isomers as $N_2O_2^-$ and $ONNO^-$, respectively, with a stability relative to DPD for reaction 1 of 2.46 eV and for reaction 2 of 1.72 eV, respectively. Combined with the known electron affinities of O and NO, these numbers further imply that the ionic bond dissociation energies are as follows:

$$N_2O_2^- \rightarrow O^- + N_2O \qquad \Delta D_0 = 1.00 \pm 0.05 \text{ eV} \quad (3)$$

$$ONNO^- \rightarrow NO^- + NO \qquad \Delta D_0 = 1.70 \pm 0.05 \text{ eV} \quad (4)$$

For these values to be accurate, two assumptions must hold. First, the anions must not be internally excited, which is generally true in the pulsed supersonic expansion ion source. This assumption will be accepted based on previous experience, although there is some evidence for a hot band in the NO + NO channel. Second, some of the products must be formed in their ground electronic, vibrational, and rotational states. This merits further consideration and, in any case, implies that these values are upper limits to the true bond dissociation energies.

The only previous study to directly investigate the bond dissociation energies of $N_2O_2^-$ was the photodissociation study in the visible wavelength region by Osborn et al.[28] Using both electron-impact and pulsed-discharge ion sources, they observed photodissociation of ions at $m/e = 60$ to both O^- + N_2O and NO + NO + e^-. Since no evidence for the production of stable NO^- ($v = 0$) was observed, they assumed NO + NO^- products were not formed in the lowest internal states, and they did not use the lower $E_{T,max}$ (and hence higher indicated bond energy) found from these data. Evidence for vibrational bending excitation in the N_2O product of reaction 3 was noted, and the observed threshold for that process was taken as the maximum E_T from which the bond dissociation energy was deduced. Assuming the presence of a single isomer, they found $\Delta D_0 =$ 1.40 eV for reaction 3 and $\Delta D_0 = 1.25$ eV for reaction 4. To explain the production of NO^- + NO from the trigonal $N_2O_2^-$ isomer, they invoked a mechanism involving rearrangement on a repulsive excited state.

As discussed above, the different photoelectron spectra observed for the two DPD channels in this experiment suggest that there are at least two isomeric forms of the anion: the trigonal $N_2O_2^-$ isomer proposed by Arnold and Neumark[23] and a strongly bound $ONNO^-$ isomer (*cis*- or *trans*-$N_2O_2^-$), with the former undergoing DPD to O + N_2O + e^- and the latter to NO + NO + e^-. It must be noted that the earlier results of Posey and Johnson,[25] who found evidence for a weakly bound $(NO)_2$ species formed in the electron impact on NO, do not exclude the possibility that a more strongly bound $ONNO^-$ anion exists. In fact, the recent calculations by Snis and Panas[9] predict that the *trans*-$ONNO^-$ anion is the most stable form of the anion, with a bond dissociation energy of 1.70 eV as opposed to 1.41 eV for the C_{2v}-$N_2O_2^-$ species.

Thus Osborn et al.[28] have reported a 1.40 eV upper limit to the bond dissociation energy for C_{2v}-N_2O_2, which agrees well with the prediction of Snis and Panas, while our results indicate 1.01 eV. On the other hand, we find a 1.70 eV bond dissociation energy for an assumed $ONNO^-$ isomer, which agrees with the stability of *trans*-$ONNO^-$ reported by Snis and Panas.[9] The NO + NO^- photodissociation data of Osborn et al. is reasonably consistent with the energetics of $ONNO^-$ reported here. As noted previously, they did not use the $N(E_T)$ observed for that channel to determine the energetics owing to the lack of evidence for the production of NO^- ($v = 0$). In any case, the results obtained here are consistent with the existence of at least two isomeric forms of $N_2O_2^-$, with the form that undergoes DPD to NO + NO + e^- being more stable than the form that yields O + N_2O + e^-. There are other potential explanations for these results, for example a single isomer with a strong state-

specific branching ratio between the two channels that leads to a markedly different partitioning of energy among the photoproducts.

An important assumption, as mentioned above, is that some ground-state products are formed in the DPD process. In this regard, it must be noted that DPD of C_{2v}-$N_2O_2^- \rightarrow O + N_2O + e^-$ would be expected to lead to significant internal excitation in the N_2O products owing to the transition from a bent O−N−N configuration (calculated to be 120° by Snis and Panas) to linear N_2O. The energy to bend N_2O to 120° is estimated to be > 1 eV,[36] so considerable bending excitation in this dissociation is expected. This leads to the question of the origin of the feature seen at low E_T in the N(E_T) and N(E_T,eKE) spectra for the $O + N_2O + e^-$ channel. Two possible product channels could give rise to this feature. The first is $O(^1D) + N_2O$. This channel lies 1.97 eV above $O(^3P) + N_2O$ and is the lowest singlet dissociation channel. As noted by Gordon and co-workers[21] and in the calculations of Arnold and Neumark,[23] there are predicted to be several singlet and triplet states of trigonal N_2O_2, and this would represent the lowest spin-allowed dissociation pathway for the singlet states. Estimating the origin of this feature in the N(E_T,eKE) spectrum as $KE_{max} = 0.8$ eV, this would yield a bond dissociation energy for trigonal $N_2O_2^- \rightarrow O^- + N_2O$ of only 0.43 eV, considerably below the prediction of Snis and Panas of the stability of this species. The second possibility is that the $N(^4S) + NO_2(^2A_1)$ channel is responsible for this feature. This channel is spin-allowed for triplet excited states. Regrettably, the photofragment mass resolution and the lack of convenient isotopic substitutions prevents a definitive assignment of this channel at this time, so the energetics must be considered. This channel lies 1.83 eV above $O(^3P) + N_2O$,[37] indicating a bond dissociation energy for trigonal-$N_2O_2^- \rightarrow O^- + N_2O$ of 0.57 ± 0.05 eV. From a Franck−Condon perspective, the $N + NO_2$ channel is more likely to produce ground-state products, as the equilibrium geometry of NO_2 has an ONO bond angle of 134.1°, closer to the ~120° ONO bond angle predicted in the various forms of trigonal N_2O_2[23] than in the case of dissociation to linear N_2O. The energetics implied by the assignment of the $N + NO_2$ dissociation pathway are also in better accord with the theoretical predictions of Snis and Panas than the $O(^1D) + N_2O$ channel.[9] The occurrence of one of these two channels, and the concomitant necessity of reducing the estimated bond dissociation energy of trigonal-$N_2O_2^-$ appears to be the simplest explanation of this additional feature in the $O + N_2O + e^-$ N(E_T) and N(E_T,eKE) spectra, although state-specific effects on the mechanism and partitioning of energy in the dissociation of the transient N_2O_2 species cannot be ruled out.

The energetics proposed for the isomeric forms of $N_2O_2^-$ and the excited states of N_2O_2 observed in this experiment are summarized in Figure 6. The neutral and ionic dissociation asymptotes are well known from the heats of formation and electron affinities for the various species.[37−39] The $ONNO^-$ anion is shown 1.70 eV below the $NO + NO^-$ asymptote, and the $N_2O_2^-$ anion is shown 0.57 eV below the $O^- + N_2O$ dissociation asymptote, consistent with the assignment of the low E_T channel to $N + NO_2 + e^-$. It is noted that the $N_2 + O_2 + e^-$ DPD pathway lies below the isomeric anions, but no evidence for kinetic energy release consistent with this low lying dissociation pathway was observed. Once the stability of the isomeric forms of the anions are fixed, the location of the neutral excited states produced by photodetachment can be assessed. As shown in the figure, the ADE of 3.35 eV for the ONNO species places it 1.63 eV above $NO + NO + e^-$, while the ADE of 3.52 eV for the N_2O_2 species places it ~2.95 eV above $NO + NO + e^-$.

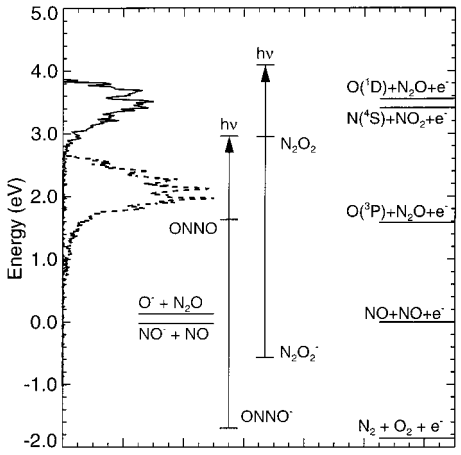

Figure 6. Energetics diagram for the DPD of $N_2O_2^-$. The 266 nm (4.66 eV) photoelectron spectra for the two channels are shown on the left plotted on an energy scale relative to the two isomers, $ONNO^-$ (dashed line) and $N_2O_2^-$ (solid line).

The location of ONNO 1.63 eV above the $NO + NO + e^-$ dissociation asymptote is in good accord with the prediction of 1.66 eV by Vincent et al.[1] for the cyclic ONNO species mentioned above. The location of the N_2O_2 neutral state accessed in this experiment, ~2.95 eV above $NO + NO + e^-$, is not reproduced as well in the calculations of Vincent et al. that found an asymmetric nearly trigonal N_2O_2 excited state 1.96 eV above $NO + NO + e^-$. The calculations of Gordon and co-workers[3] found at least five N_2O_2 minima between 1.5 and 3.0 eV above this asymptote. Arnold and Neumark studied a number of singlet and triplet states of trigonal N_2O_2 and found both a C_s symmetry $^1A'$ and a trigonal C_{2v} symmetry $^3A_2$ state ~1.6 eV above $NO + NO + e^-$.[23] Given the number of low-lying excited states, it is difficult to make a definitive assignment based on the calculations and the present experimental results.

As noted in the Introduction, isotopically labeled studies of the $O^- + N_2O \rightarrow NO^- + NO$ reaction have shown that there is a common intermediate where isotope scrambling occurs.[30,31] Our results show that there are two distinct isomeric forms, but do not shed light on the barrier to interconversion between these forms. As the ions are formed in a supersonic expansion, the vibrational temperature is typically found to be on the order of 300−500 K, so it is very possible that the trigonal $N_2O_2^-$ species may be transient in reaction processes, with isotopic scrambling occurring upon conversion of trigonal $N_2O_2^-$ to the more stable $ONNO^-$ anion.

C. Excited-State Dissociation Dynamics. The dissociation of the ONNO species to NO + NO is characterized by a large kinetic energy release with no evidence for product NO vibrational state resolution in the N(E_T) or N(E_T,eKE) spectra. Once this species crosses to a dissociative surface there is considerable repulsion between the NO products, and given the 1900 cm^{-1} vibrational frequency in the NO products, the lack of vibrational resolution shows that there is significant rotational excitation in this dissociation. As discussed above, a cyclic ONNO species calculated by Vincent et al. is consistent with the energetics found in this experiment.[1] This species, also found in lower-level MP2 calculations by Gordon and co-workers, is not a perfect rectangle, thus considerable rotational excitation in the dissociation is expected, unlike the O_4^- system previously studied in this laboratory in which vibrationally resolved correlation spectra were observed.[40]

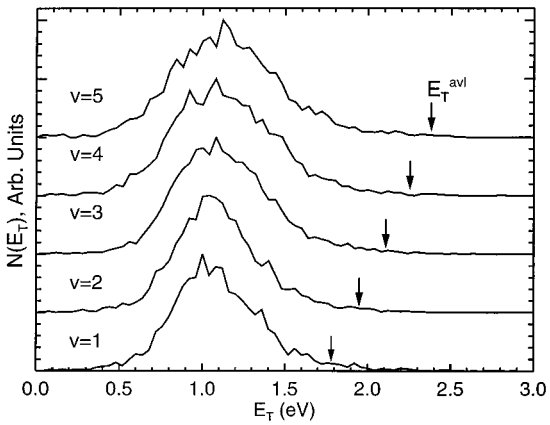

Figure 7. The photofragment translational energy distributions for the different vibrational states of the transient ONNO molecule in the NO + NO + e^- product channel. These spectra were generated from the N(E_T,eKE) spectrum by integrating 0.1 eV wide slices centered on the peaks in the N(eKE) spectrum for NO + NO + e^- in Figure 2b. The arrows indicate the maximum available translational energy, E_T^{avl}, for the NO + NO products as determined by energy conservation and the measurement of the photoelectron kinetic energy.

The photofragment N(E_T) distributions for the different vibrational states of the transient ONNO molecule can be determined by examining eKE-gated slices of the N(E_T,eKE) spectrum in Figure 4 around the peaks resolved in the N(eKE) spectrum for this channel. The results are shown in Figure 7, in which the arrows indicate the maximum available energy for internal and translational degrees of freedom of the NO products. The peak positions in the N(E_T) spectra for $v = 1-5$ are nearly identical, so conservation of energy in this coincidence experiment dictates that the peak internal energy among the NO + NO products increases linearly with excitation in the ONNO neutral, as determined by the eKE measured in coincidence. Going from $v = 1$ up to 5, the peak E_T increases slightly from 1.0 to 1.1 eV, but the fraction of the available energy appearing in translation at the peak decreases from 56% to 46% over this range. It is intriguing that nearly the same peak E_T is observed for the dissociation of these different vibrational states of ONNO. Generally in DPD experiments it is assumed that the peak E_T is a measure of the repulsion between the photofragments upon crossing to the dissociative surface, as shown in the vibrationally resolved experiments on the direct DPD of O_4^-.[40] In the case of the sequential DPD of O_3^-, which exhibits a structured photoelectron spectrum similar to $ONNO^-$, a greater variation of the N(E_T) distribution with eKE was observed, although the trend was similar in that higher internal excitation in the nascent O_3 led to higher internal excitation among the photofragments.[41] Further characterization of the dissociative surfaces involved will be necessary to resolve this question.

As discussed above, the O + N_2O + e^- channel is assigned to DPD of the $N_2O_2^-$ isomer. Given the broad, poorly resolved structure observed in this photoelectron spectrum, this dissociation pathway may proceed very rapidly with concomitant lifetime broadening in the photoelectron spectrum. The eKE resolution in these experiments, however, precludes a definitive answer at this time. Similar to the NO + NO channel, a large E_T release is observed at the peak of the N(E_T) distribution, indicative of significant repulsion between the O + N_2O products. As discussed above, a possible candidate for the N_2O_2 state here is the C_s symmetry $^1A'$ state. Dissociation of this state to O(^3P) + N_2O is spin-forbidden. However, Gordon and coworkers[21] have predicted that this C_s-N_2O_2 ($^1A'$) species rapidly predissociates to N_2O ($X\ ^1\Sigma^+$) + O (^3P) by spin−orbit interactions. The current study also provides evidence for a second dissociation pathway to N(^4S) + NO_2 ($^2A_1$) for the N_2O_2 species. This dissociation pathway is only spin-allowed from a triplet state, possibly the $^3A_2$ state predicted by Arnold and Neumark in the same energy range as the $^1A'$ state. Spin-allowed dissociation of the $^1A'$ state to yield O (^1D) + N_2O products is also energetically possible, as discussed above. One of these two dissociation pathways could be responsible for the low E_T feature, with energetic considerations favoring the N(^4S) + NO_2 channel.

5. Conclusion

The DPD of $N_2O_2^-$ has been studied at 266 nm, revealing two major dissociative photodetachment channels, ONNO → NO + NO + e^- and N_2O_2 → O + N_2O + e^-. PPC spectroscopy allows separation of the photoelectron spectrum into contributions from these channels, and the observed energetics imply the existence of at least two distinct isomers of $N_2O_2^-$. The results are consistent with an $ONNO^-$ species stable relative to NO + NO + e^- by $< 1.70 \pm 0.05$ eV, while trigonal $N_2O_2^-$ is stable relative to O^- + N_2O by $< 0.57 \pm 0.05$ eV. The energetics of the trigonal $N_2O_2^-$ are fixed by the assignment of a low-energy feature in the correlation spectra to the N(^4S) + NO_2 product channel. The rapid dissociation of all the excited states of N_2O_2 observed in these photodetachment experiments indicates that these species are not good candidates for high-energy density materials. In addition, this study demonstrates the insights into multiple isomeric species and dissociation channels to be gained from photoelectron-photofragment coincidence spectroscopy. There remains much work to be done, however, in both the experimental and theoretical characterization of the rich excited-state chemistry of N_2O_2.

Acknowledgment. This work was supported by the Air Force Office of Scientific Research under Grants F49620-96-1-0220 and F49620-000-10-010. R.E.C. is a Camille Dreyfus Teacher-Scholar and acknowledges the support of a Packard Fellowship in Science and Engineering and an Alfred P. Sloan Research Fellowship.

References and Notes

(1) Vincent, M. A.; Hillier, I. H.; Salsi, L. *Phys. Chem. Chem. Phys.* **2000**, *2*, 707.
(2) Snis, A.; Panas, I. *Surf. Sci.* **1998**, *412/413*, 477.
(3) Nguyen, K. A.; Gordon, M. S.; Montgomery, J. A.; Michels, H. H. *J. Phys. Chem.* **1994**, *98*, 10072.
(4) Nour, E. M.; Chen, L.-H.; Strube, M. M.; Laane, J. *J. Phys. Chem.* **1984**, *88*, 756.
(5) Brechignac, P.; De Benedictis, S.; Halberstadt, N.; Whitaker, B. J.; Avrillier, S. *J. Chem. Phys.* **1985,** *83*, 2064.
(6) McKellar, A. R. W.; Watson, J. K. G.; Howard, B. J. *Mol. Phys.* **1995**, *86*, 273.
(7) Strobel, A.; Knoblauch, N.; Agreiter, J.; Smith, A. M.; Niedner-Schatteburg, G.; Bondybey, V. E. *J. Phys. Chem.* **1995**, *99*, 872.
(8) Blanchet, V.; Stolow, A. *J. Chem. Phys.* **1998**, *108*, 4371.
(9) Snis, A.; Panas, I. *Chem. Phys.* **1997**, *221*, 1.
(10) Harcourt, R. D. *J. Mol. Struct. (Theochem.)* **1990**, *206*, 253.
(11) Kishner, S.; Whitehead, M. A.; Gopinathan, M. S. *J. Am. Chem. Soc.* **1978**, *100*, 1365.
(12) Phillips, L. F.; Schiff, H. I. *J. Chem. Phys.* **1965**, *42*, 3171.
(13) Iwata, R.; Ferrieri, R. A.; Wolf, A. P. *J. Phys. Chem.* **1986**, *90*, 6722.
(14) Ross, S. K.; Sutherland, J. W.; Kuo, S.-C.; Klemm, R. B. *J. Phys. Chem. A* **1997**, *101*, 1104.
(15) Last, I.; Aguilar, A.; Sayós, R.; González, M.; Gilibert, M. *J. Phys. Chem. A* **1997**, *101*, 1206.
(16) Brouard, M.; Duxon, S. P.; Enriquez, P. A.; Simons, J. P. *J. Chem. Phys.* **1992**, *97*, 7414.
(17) Pisano, P. J.; Westley, M. S.; Houston, P. L. *Chem. Phys. Lett.* **2000**, *318*, 385.

(18) Yang, X.; Price, J. M.; Mack, J. A.; Morgan, C. G.; Rogaski, C. A.; McGuire, D.; Kim, E. H.; Wodtke, A. M. *J. Phys. Chem.* **1993**, *97*, 3944.
(19) Bardo, R. D. *J. Phys. Chem.* **1982**, *86*, 4658.
(20) Zandwijk, V. G.; Janssen, R. A. J.; Buck, H. M. *J. Am. Chem. Soc.* **1990**, *112*, 4155.
(21) (a) Nguyen, K. A.; Gordon, M. S.; Boatz, J. A. *J. Am. Chem. Soc.* **1994**, *116*, 9241. (b) Chaban, G.; Gordon, M. S.; Nguyen, K. A. *J. Phys. Chem. A* **1997**, *101*, 4283. (c) Nguyen, K. A.; Gordon, M. S.; Montgomery, J. A.; Michels, H. H.; Yarkony, D. R. *J. Chem. Phys.* **1992**, *98*, 3845.
(22) Michels, H. H.; Montgomery, J. A. *J. Chem. Phys.* **1988**, *88*, 7248.
(23) Arnold, D. W.; Neumark, D. M. *J. Chem. Phys.* **1995**, *102*, 7035.
(24) Naitoh, Y.; Fujimura, Y.; Honma, K.; Kajimoto, O. *J. Phys. Chem.* **1995**, *99*, 13652.
(25) Posey, L. A.; Johnson,M. A. *J. Chem. Phys.* **1988**, *88*, 5383.
(26) (a) Jacox, M. E.; Thompson, W. E. *J. Chem. Phys.* **1990**, *93*, 7609. (b) Jacox, M. E. *J. Chem. Phys.* **1990**, *93*, 7622.
(27) Hacaloglu, J.; Suzer, S.; Andrews, L. *J. Phys. Chem.* **1990**, *94*, 1759.
(28) Osborn, D. L.; Leahy, D. J.; Cyr, D. R.; Neumark, D. M. *J. Chem. Phys.* **1996**, *104*, 5026.
(29) Van Doren, J. M.; Barlow, S. E.; DePuy, C. H.; Bierbaum, V. M. *J. Am. Chem. Soc.* **1987**, *109*, 4412.
(30) Morris, R. A.; Viggiano, A. A.; Paulson, J. F. *J. Chem. Phys.* **1990**, *92*, 3448.
(31) Barlow, S. E.; Bierbaum, V. M. *J. Chem. Phys.* **1990**, *92*, 3442.
(32) Duarte, H. A.; Proynov, E.; Salahub, D. R. *J. Chem. Phys.* **1998**, *109*, 26.
(33) East, A. L. L. *J. Chem. Phys.* **1998**, *109*, 2185.
(34) Hanold, K. A.; Sherwood, C. R.; Garner, M. C.; Continetti, R. E. *Rev. Sci. Instrum.* **1995**, *66*, 5507.
(35) Sherwood, C. R.; Hanold, K. A.; Garner, M. C.; Strong, K. M.; Continetti, R. E. *J. Chem. Phys.* **1996**, *105*, 10803.
(36) Ferguson, E. F.; Fehsenfeld, F. C.; Schmeltekopf, A. L. *J. Chem. Phys.* **1967**, *47*, 3085.
(37) Chase, M. W.; Davies, C. A.; Downey, J. R.; Frurip, D. J.; McDonald, R. A.; Syverud, A. N. *J. Phys. Chem. Ref. Data Suppl. 1*, **1985**, *14*.
(38) Neumark, D. M.; Lykke, K. R.; Anderson, T.; Lineberger,W. C. *Phys. Rev. A* **1985**, *32*, 1890.
(39) Travers, M. J.; Cowles, D. C.; Ellison, G. B. *Chem. Phys. Lett.* **1989**, *164*, 449.
(40) Hanold, K. A.; Continetti, R. E. *Chem. Phys.* **1998**, *239*, 493.
(41) Garner, M. C.; Hanold, K. A.; Resat, M. S.; Continetti, R. E. *J. Phys. Chem. A* **1997**, *101*, 6577.